Series: ELECTRONICS, COMPUTERS and ARTIFICIAL INTELLIGENCE – ECAI-2013

Contents

Vol. 5 – No. 1/ 2013 ISSN – 1843 – 2115

Media	IEEE Catalog Number	ISBN
Compliant PDF Files	CFP1327U-ART	978-1-4673-4937-6
DVD	CFP1327U-DVD	978-1-4673-4936-9
Print	CFP1327U-PRT	978-1-4673-4935-2

UNIVERSITY OF PITESTI

Technical sponsorship

IEEE Region 8

IEEE Industry Applications Society

Proceedings of the International Conference on ELECTRONICS, COMPUTERS and ARTIFICIAL INTELLIGENCE – ECAI-2013

Series: ELECTRONICS, COMPUTERS and ARTIFICIAL INTELLIGENCE

Vol. 5 – No. 1/ 2013 ISSN – 1843 – 2115

Media	IEEE Catalog Number	ISBN
Compliant PDF Files	CFP1327U-ART	978-1-4673-4937-6
DVD	CFP1327U-DVD	978-1-4673-4936-9
Print	CFP1327U-PRT	978-1-4673-4935-2

ECAI 2013 - International Conference – 5th Edition
Electronics, Computers and Artificial Intelligence
27 June -29 June, 2013, Pitesti, ROMÂNIA

On the search speed for the extremum seeking control 2D-schemes. Part II – signal processing using orthogonal dither signals

Nicu Bizon[1)2)], Mihai Oproescu[1)], Marian Raducu[1)], Luminita Mirela Constantinescu[1)]
[1)]University of Pitesti, 1 Targu din Vale, Arges, 110040 Pitesti, Romania, nicubizon@yahoo.com ; nicu.bizon@upit.ro; Tel +40 348 453 201, Fax +40 348 453 200
[2)] University Politehnica of Bucharest, 313 Splaiul Independentei, 060042 Bucharest, Romania

Abstract **In this paper an analysis of the Extremum Seeking Control (ESC) 2D-scheme for the dual-inputs single-output (DISO) systems is presented. The ESC 2D-schemes have two loops where the output signal is processed based on the different ESC algorithms proposed in the literature. The basic high-order ESC (bhoESC) 2D-scheme and an improved ESC variant will be analyzed here based on the two orthogonal dither signals. The proposed ESC scheme is based on a band-pass filter (BPF) instead of the series combination of high-pass (HP) and low-pass (LP) filters used in the bhoESC scheme. The processing of the output signal shows that the search speed in both bpfESC loops depends on the BPF cut-off frequencies. So, besides the gradient signals, the injected signals on the both bhoESC inputs contain the Low Frequencies (LF) components from the BPF band. Thus the dither persistence in the bpfESC loops is improved in comparison with the bhoESC scheme. The relations between the search speeds and the partial derivatives of an unknown DISO map are shown.**

Keywords: nonlinear DISO system, extremum seeking control, search speed, signal processing, MPP tracking

1. INTRODUCTION

In general, a nonlinear dynamic DISO system has an unknown map, $y=f(x_1, x_2)$, having one or more extremes (maximums or minimums). Searching and tracking the global optimum of a nonlinear dynamic DISO map is a challenging task that could involve a large number of functional evaluations [1, 2].

The ESC algorithms differ in their gradient estimation methods. The dither gradient estimation approach will be discussed in this paper [1]. In the classical methods, including the bhoESC scheme, a temporal variation, i.e., a dither signal with constant (pre-fixed amplitude) is added to input. The gradient is obtained as a correlation between the inputs and the output. As an alternative, an improved bpfESC scheme is proposed and applied to harvest the energy from the Photovoltaic (PV) panels [3] and Fuel Cells (FC) stacks [4]. In this paper, the bpfESC 2D-scheme, which can be used for example to improve the energy harvested from a FC stack based on control of both fuelling rates, will be analyzed. The air control is shown in [5] based on bhoESC scheme applied to the motocompressor group. Also, the hydrogen control is shown in [4] based on bpfESC 1D-scheme.

In this paper the search speeds related to the both inputs will be estimated during the search phase for a bpfESC 2D-scheme, and these will be compared with those obtained with the bhoESC 2D-scheme. So, this paper will concern itself with the ESC schemes discussed in [1, 4], being focused only on the analysis of the ESC 2D-schemes in order to evaluate the search speeds. In addition, the used bpfESC 1D-scheme is topologically improved to increase both search speed and tracking accuracy, which are the main indicators used to evaluate the performance of the ESC algorithms [6]. Other different approaches are shown in the literature [7, 8], but these are more complicated than the bpfESC 2D-scheme proposed here. If the integrator, that is a key adaptation element in all ESC schemes, is already present in the transfer function of the system, then this can be used to simplify the topology of the ESC loop for the 2D schemes [9].

Note that the classical ESC approach for DISO and MIMO systems is defined for example in [10] and [11], respectively. The stability results obtained in this paper can be proved based on the techniques introduced in [12, 13].

The paper is organized as follows. Section 2 presents in brief the ESC 1D-schemes used in simulation. This aspect is briefly shown in this section. Section 3 deals with the ESC 2D-schemes based on the orthogonal dither signals. An analytical analysis of the ESC 2D-scheme in the frequency domain is presented based on Taylor series approximation. The main analytical results obtained by estimating the search speeds are shown for both ESC 2D-schemes. The performance of the bpfESC scheme related to the search speeds is

clearly highlighted. The last section concludes the paper.

2. THE EXTREMUM SEEKING CONTROL 1D-SCHEMES BASED ON SINUSOIDAL DITHER SIGNALS

A brief analysis of the ESC 1D-scheme (Figure 1) based on the sinusoidal dither signals [14] is performed in this section. If the transfer function of the BP filter from the bpfESC scheme is equivalent with the series combination of the High-Pass (HP) and the Low-Pass (LP) filters from the ho ESC scheme, then the hoESC and bpfESC schemes are functionally equivalent, too. It can be observed that both ESC 1D-schemes have the same operating relationships, excepting the signal filtering and demodulation [1, 3]. Thus, considering $G_{BPF}(s) = G_{BPF}(s) = G_{HPF}(s)\cdot G_{LPF}(s) = [Y_{BPF}(s)/ Y_F(s)] \cdot [Y_F(s)/ Y_N(s)] = [s/(s + \omega_h)]\cdot[\omega_l/(s + \omega_l)]$, the equivalent operation of the bpfESC and hoESC 1D schemes was demonstrated in [15].

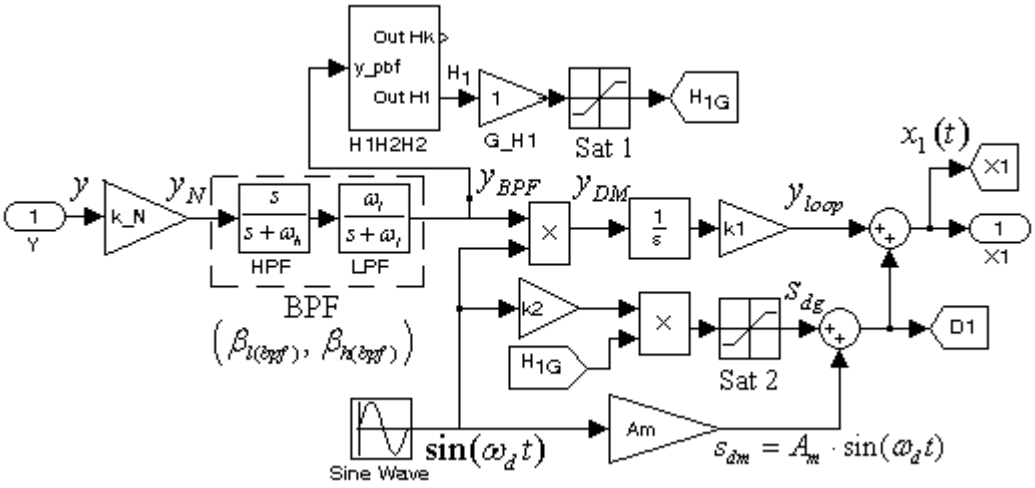

Fig. 1a. The BPF extremum seeking control (bpfESC) 1D scheme

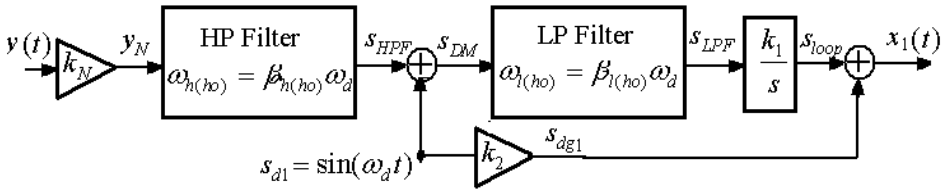

Fig. 1b. The higher order extremum seeking (hoESC) 1D scheme

2.1. The bpfESC 1D-scheme

Using only the measurements of the plant output, y (for example, the power signal from the PV panel or FC stack), the ESC schemes perform a tuning of the plant input, x_1, such that $y=f(x_1)$ is either minimized or maximized. The initial value, x_{01}, must be set in the region of the MPP attraction to assure $y \in y_{MPP}$.

The relationships of the bpfESC scheme are shown below [1, 3]

$$y = f(x_1),\ y_N = k_N \cdot y \quad (1)$$

$$\dot{y}_F = -\omega_h y_F + \omega_h y_N,\ y_{BPF} = y_N - y_F,\ \dot{y}_{BPF} = -\omega_l y_{BPF} + \omega_l y_F,\ y_{DM} = y_{BPF}\cdot\sin(\omega_d t) \quad (2)$$

$$\dot{y}_{loop} = k_1 y_{DM} \quad (3)$$

$$x_1 = y_{loop} + s_{dg} + s_{dm},\ s_{dg} = k_2 H_1 G_{H1}\cdot\sin(\omega_d t),\ s_{dm} = A_m\cdot\sin(\omega_d t) \quad (4)$$

where equations (1), (3), and (4) represent the input-to-output map, integrator, MPP current controller based on the x_{in} reference, and equations (2) represent the signal processing based on BPF and demodulation.

The following notations are used (see Figure 1a):

- k_1 is the loop gain;
- ω_d is the frequency of the dither signal;
- $\omega_l=\beta_l\omega_d$, $3<\beta_l<6$, is the cut-off frequency of the LPF;
- $\omega_h=\beta_h\omega_d$, $0<\beta_h<1$, is the cut-off frequency of the HPF;
- y_N is the signal after normalization (with the k_N gain);
- y_F is an intermediate variable related to HPF operating;
- y_{BPF} is the output signal from the BPF;
- H_1 is the magnitude of the fundamental harmonic of the y_{BPF} signal;
- G_{H1} is the gain of the H_1 harmonic;
- s_{dg} is the gained dither;
- $k_2H_1G_{H1}$ is the gain of the s_{dg} dither;
- s_{dm} is the minimum dither;
- A_m is the amplitude of the s_{dm} dither;
- y_{DM} is the signal after demodulation;
- y_{loop} is the output signal from the bpfESC loop;

- x_1 and x_2 are the estimation signals of the unknown parameters;

2.2. The hoESC 1D-scheme

Relationships of the hoESC 1D-scheme (Figure 1b) related to the signal processing based on the BP and HP filters and demodulation are [1]:

$$\dot{s}_F = -\omega_h s_F + \omega_h s_N, \quad s_{HPF} = s_N - s_F, \quad \dot{s}_{LPF} = -\omega_l s_{LPF} + \omega_l s_{HPF} \sin(\omega t) \tag{5}$$

where s_N, s_{HPF}, and s_{LPF} are the signals after normalization, HPF, and LPF, besides the notations used for the bpfESC 1D-scheme. Also:

- $\omega_{l(ho)}=\beta_{l(ho)}\omega_d$, $0<\beta_{l(ho)}<6$, is the cut-off frequency of the $LPF_{(ho)}$;
- $\omega_{h(ho)}=\beta_{h(ho)}\omega_d$, $0<\beta_{h(ho)}<1$, is the cut-off frequency of the $HPF_{(ho)}$.

The injected signal will be:

$$x_1 = s_{loop} + k_2 \cdot \sin(\omega_d t) \tag{6}$$

where sloop is the output signal from the hoESC loop that is obtained after integrator block.

If the cut-off frequencies of the filters used are almost the same for both ESC 1D schemes ($\beta_{l(ho)} \cong \beta_{l(bpf)}$ and $\beta_{h(ho)} \cong \beta_{h(bpf)}$), then the same search speed will be obtained [15]. On the other hand, if the cut-off frequency of the $LPF_{(ho)}$ is lower than the dither frequency ($0<\beta_{l(ho)}<1$), then this basic hoESC variant (bhoESC) will have a lower search speed in comparison to the bpfESC 1D scheme [15].

The bhoESC and bpfESC 1D scheme will be combined to obtain the corresponding bhoESC and bpfESC 2D-schemes, based on the orthogonal dither signals.

3. THE ESC 2D-SCHEMES BASED ON ORTHOGONAL DITHER SIGNALS

In this section, the ESC 2D-schemes for systems with dual inputs and one output (DISO systems) will be presented. The principle of the ESC for the multi-inputs one-output (MISO) systems [11], including the particular case of the DISO systems [9, 10], is very similar to the SISO case. The orthogonal dither signals are superimposed on both inputs, x_1 and x_2 (see Figure 2). The local gradients $\partial f/\partial x_1$ and $\partial f/\partial x_2$ are estimated in both ESC loops (see Figure 3) based on demodulation of the filtered output, y_{BPF}. The y_{BPF} signal is obtained through BP filtering of the normalized probing signal, y_N. The probing signal is obtained as a response of the LF signals, $x_{1(LF)}$ and $x_{2(LF)}$, applied to the nonlinear map, $y=f(x_1, x_2)$. For the estimation of the each gradient, the classical combination of HP and LP filters as described in Section 2.2 (see Figure 1) or a BP filter as described in Section 2.1 (see Figure 1) can be used.

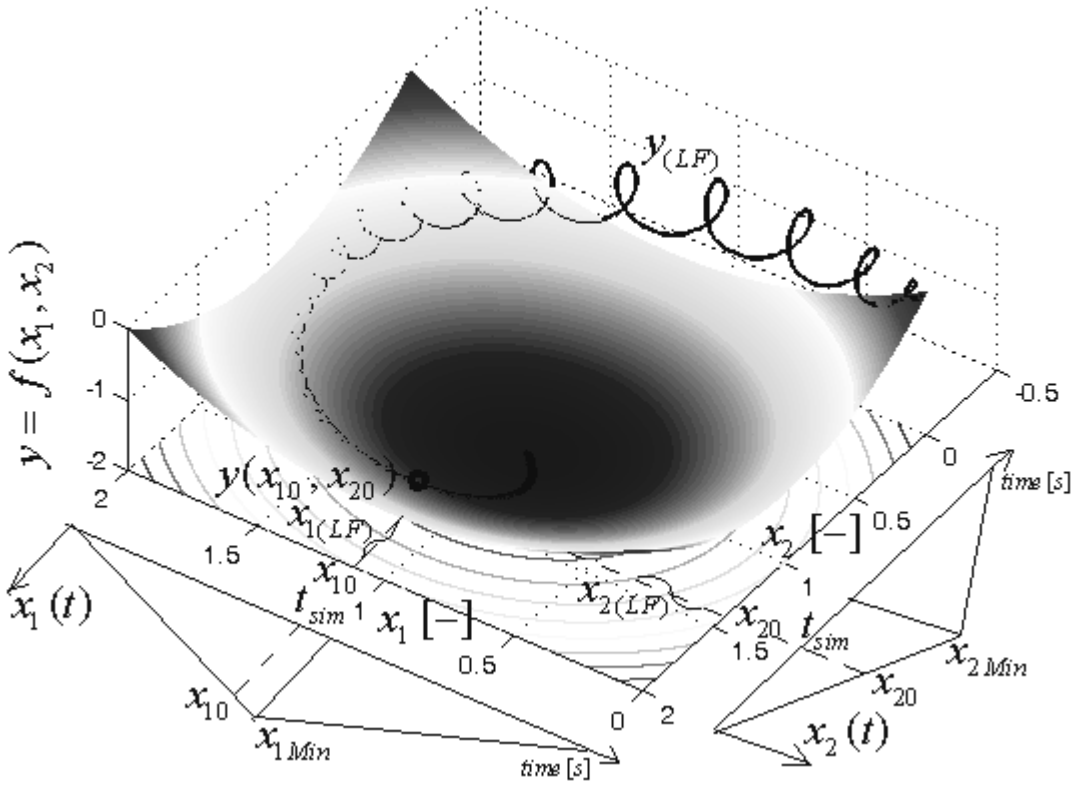

Fig. 2. Searching of the MPP based on dither signal ESC 2D scheme

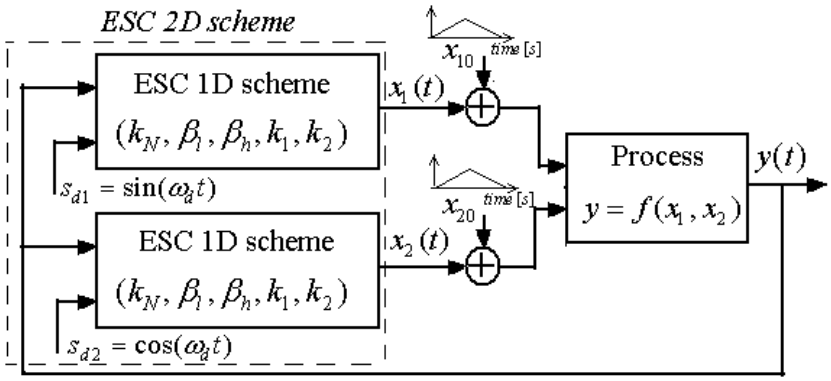

Fig.3. The ESC 2D scheme operating in closed loop

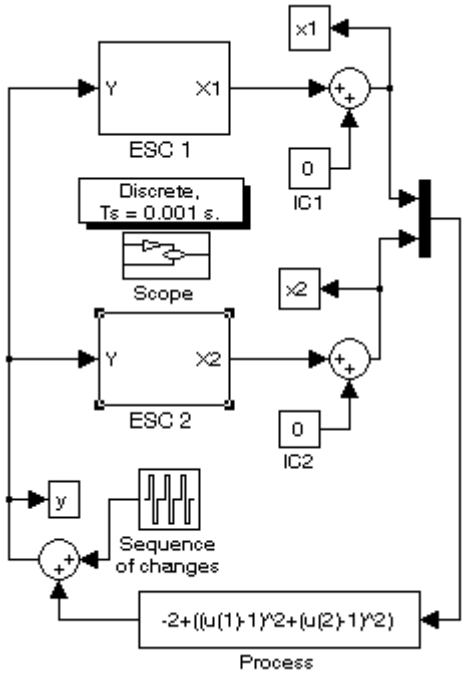

Fig. 4. The diagram for testing the ESC 2D schemes using different process in the closed loop

As it was explained in the previous sections, besides the LF components from the demodulation signal, x_{DM}, each gradient drives an integrator, obtaining the time-variable signals that move the inputs x_1 and x_2 towards their optimal values (x_{1Min} and x_{2Min} in case of Figure 2).

3.1. Signal processing in the bpfESC 2D-scheme loops

The probing signal related to the nonlinear map, $y=f(x_1, x_2)$, can be approximated by the Taylor series:

$$y(x_1, x_2) = \sum_{i_2=0}^{\infty} \left(\sum_{i_1=0}^{\infty} \frac{(x_1 - x_{10})^{i_1} (x_2 - x_{20})^{i_2}}{i_1! i_2!} \cdot \frac{\partial^{i_1+i_2} f}{\partial x_1^{i_1} \partial x_2^{i_2}} (x_{10}, x_{20}) \right) \quad (7)$$

where (x_{10}, x_{20}) is a point that slowly varies in time as it is shown in Figure 2, and $y_0=f(x_{10}, x_{20})$ is an output value based on the 2D static map. If the start point is considered the point (0, 0), then the ramp for $t<t_{MPP}$ is given by relationship:

$$x_{p0}(t) = \frac{x_{pMPP}}{t_{MPP}} \cdot t = G_p \cdot t, \quad p = 1, 2 \quad (8)$$

Note that t_{MPP} is the time of simulation and G_p, p=1, 2, are the slopes of ramps used to test the nonlinear plant in the open loop. The gradients, K_{SS1} and K_{SS2}, can be estimated in closed loop based on:

$$K_{SS(p)} = \frac{\partial f}{\partial x_p}(x_{10}, x_{20}) = \frac{df}{dt} / \frac{dx_p}{dt}, \quad p = 1, 2 \quad (9)$$

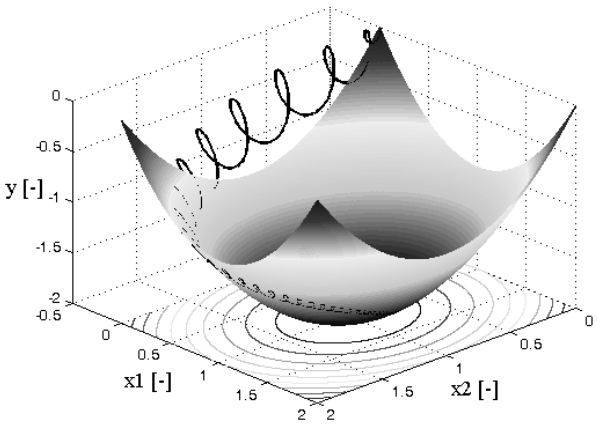

Fig. 5. The 3D view of the search phase for the ESC 2D scheme applied to the process $y=-2-(1-x_1)^2-(1-x_2)^2$: f_d=10 Hz

The main LF components in both loops of the bpfESC 2D-scheme are obtained as an effect of the distortion and phase shift of the dither signals applied to the nonlinear process. The dither used are orthogonal signals, $s_{d1}=\sin(\omega_d t)$ and $s_{d2}=\cos(\omega_d t)$, and numbers of harmonics will be set by the cut-off frequencies of the BPF. So, the LF signal in the ESC loop will be given by the relationship:

$$x_{LF}(t)=\sum_{j=1}^{[\beta_l]} a_j \sin(j\omega_d t+\varphi_j) \tag{10}$$

where the integer $[\beta_l]$ was set to 3 in order to simplify the presentation.

The magnitudes of the LF components, a_j and b_j, are lower than the x_0 value, so:

$$x_p=x_{p0}+x_{LF}\cong x_{p0}\Rightarrow \frac{dx_p}{dt}\cong\frac{dx_{p0}}{dt},\ p=1,2 \tag{11}$$

Consequently:

$$y_N(t)\cong k_N\sum_{i_2=0}^{\infty}\sum_{i_1=0}^{\infty}\left\{\left[x_{LF}(t)\right]^{i_1+i_2}\cdot\frac{1}{i_1!i_2!}\cdot\frac{\partial^{i_1+i_2}f}{\partial x_1^{i_1}\partial x_2^{i_2}}(x_{10},x_{20})\right\} \tag{12}$$

3.2. Estimation of the search speed in the bpfESC 2D-scheme loops

Estimation of the search speed in closed loop of the bpfESC 2D-scheme will be performed considering the following assumptions:

- only three components of the Taylor series will be considered;
- the BPF is ideal, having $\beta_{h(bpf)}<1$ and $3<\beta_{l(bpf)}<4$;
- $k_N=1$ (in simulation $k_N=1/y_{max}$).

Under these conditions the relationship of the y_{BPF} signal will be:

$$y_{BPF}(t)\cong D_1\cdot x_{LF}(t)+\frac{1}{2}D_2\cdot x_{LF}^2(t)+\frac{1}{6}D_3\cdot x_{LF}^3(t)=\\ =\sum_{i=1}^{3}\frac{1}{i!}D_i\cdot x_{LF}^i(t) \tag{13}$$

where:

$$\begin{aligned}D_1&=\frac{\partial f}{\partial x_1}(x_{10},x_{20})+\frac{\partial f}{\partial x_2}(x_{10},x_{20})\\ D_2&=\frac{\partial f^2}{\partial x_1^2}(x_{10},x_{20})+2\frac{\partial f^2}{\partial x_1\partial x_2}(x_{10},x_{20})+\\ &+\frac{\partial f^2}{\partial x_2^2}(x_{10},x_{20})\\ D_3&=\frac{\partial f^3}{\partial x_1^3}(x_{10},x_{20})+3\frac{\partial f^3}{\partial x_1^2\partial x_2}(x_{10},x_{20})+\\ &+3\frac{\partial f^3}{\partial x_1\partial x_2^2}(x_{10},x_{20})+\frac{\partial f^3}{\partial x_2^3}(x_{10},x_{20})\end{aligned} \tag{14}$$

The signals after the demodulation are:

$$\begin{aligned}y_{DM1}(t)&=y_{BPF}(t)\cdot\sin(\omega_d t)\\ y_{DM2}(t)&=y_{BPF}(t)\cdot\cos(\omega_d t)\end{aligned} \tag{15}$$

Using trigonometric manipulation, more or less complex, these signals can be written as:

$$\begin{aligned}y_{DM1}(t)&\cong k_{sg1}+y_{DM1(LF)}(t)\\ y_{DM2}(t)&\cong k_{sg2}+y_{DM2(LF)}(t)\end{aligned} \tag{16}$$

where:

$$\begin{aligned}k_{sg1}&=\frac{1}{2}D_1a_1\cos\varphi_1\cdot\left[1+\frac{1}{8}\frac{D_3}{D_1}\left(a_1^2+2a_2^2+2a_3^2\right)\right]\\ k_{sg2}&=\frac{1}{2}D_1a_1\sin\varphi_1\cdot\left[1+\frac{1}{8}\frac{D_3}{D_1}\left(a_1^2+2a_2^2+2a_3^2\right)\right]\end{aligned} \tag{17}$$

In both cases, the derivatives can be computed during the simulation based on the relationship (9): Thus, the signal injected in the loop will be:

$$\begin{aligned}x_1(t)&\cong k_1k_{sg1}\cdot t+k_2H_1G_{H1}\sin(\omega_d t)+x_{1(LF)}(t)\\ x_2(t)&\cong k_1k_{sg2}\cdot t+k_2H_1G_{H1}\cos(\omega_d t)+x_{2(LF)}(t)\end{aligned} \tag{18}$$

where H_1 is the magnitude of the fundamental harmonic of the y_{BPF} signal and G_{H1} is its gain.

The LF components after demodulation are integrated and then injected in the closed loop of the bpfESC 2D-scheme, assuring the dither persistence.

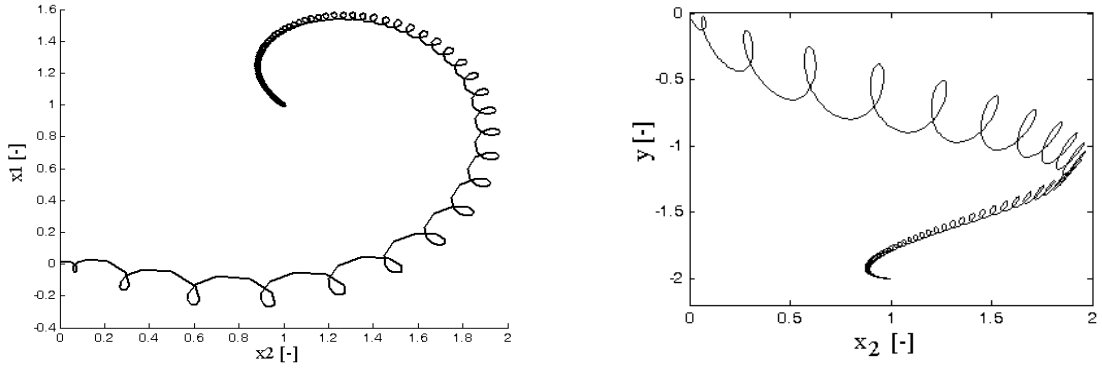

a) projection in (x_1, x_2) plane b) projection in (y, x_2) plane

Fig. 6. The 2D projections of the search 3D line for the ESC 2D scheme applied to the process $y=-2-(1-x_1)^2-(1-x_2)^2$: f_d=10 Hz

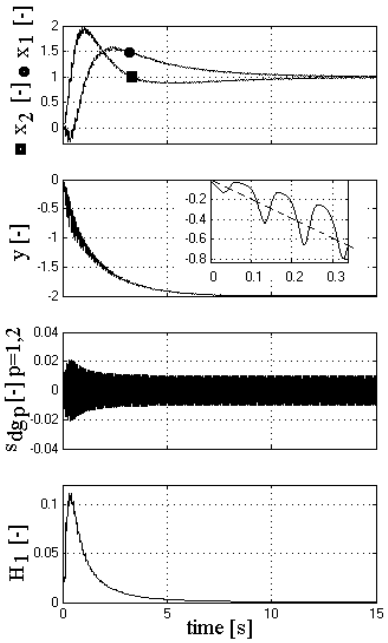

a) f_d=10 Hz

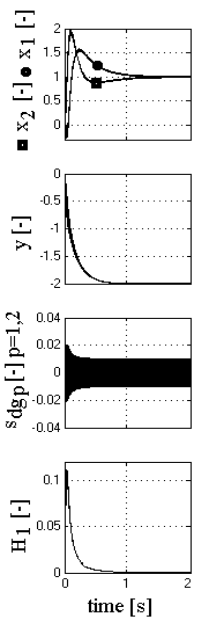

b) f_d=100 Hz

Fig. 7. The search phase the ESC 2D scheme applied to the process $y=-2-(1-x_1)^2-(1-x_2)^2$

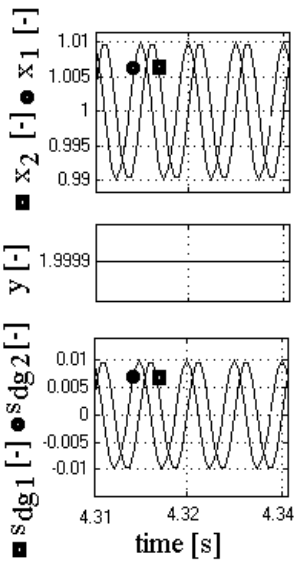

Fig. 8. Zooms of the tracking accuracy the ESC 2D scheme applied to the process $y=-2-(1-x_1)^2-(1-x_2)^2$: f_d=100 Hz

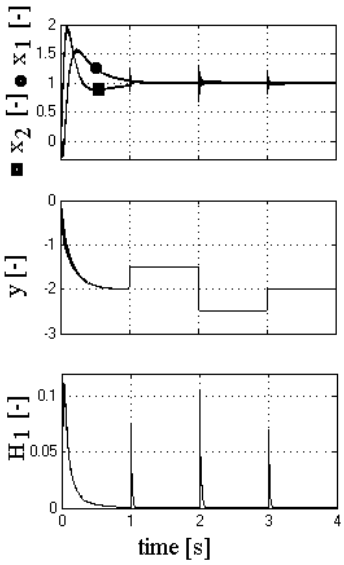

Fig. 9. The search phase for the ESC 2D scheme applied to the perturbed process $y=\pm0.5-2-(1-x_1)^2-(1-x_2)^2$: f_d=100 Hz

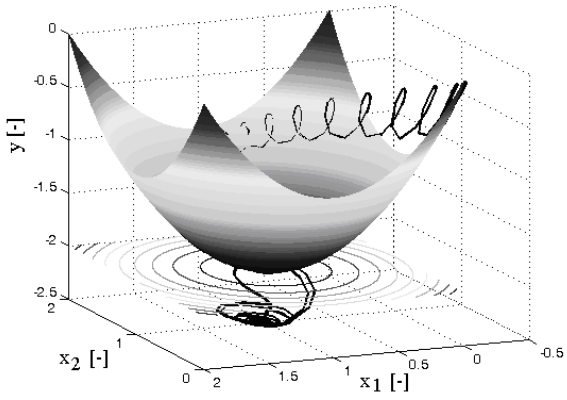

a) The 3D line on the basic process (unperturbed)

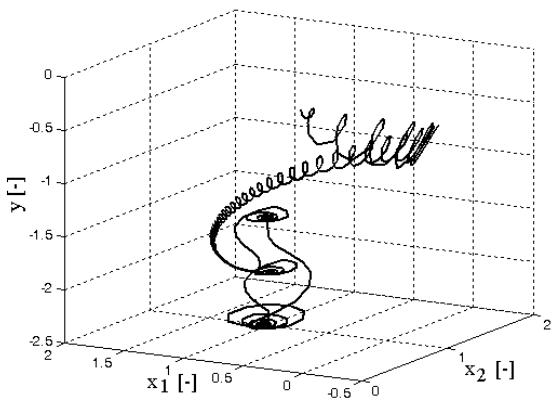

b) The 3D line is shown in a different perspective

Fig. 10. The 3D view of the search phase for the ESC 2D scheme applied to the perturbed process $y=\pm0.5-2-(1-x_1)^2-(1-x_2)^2$: f_d=100 Hz

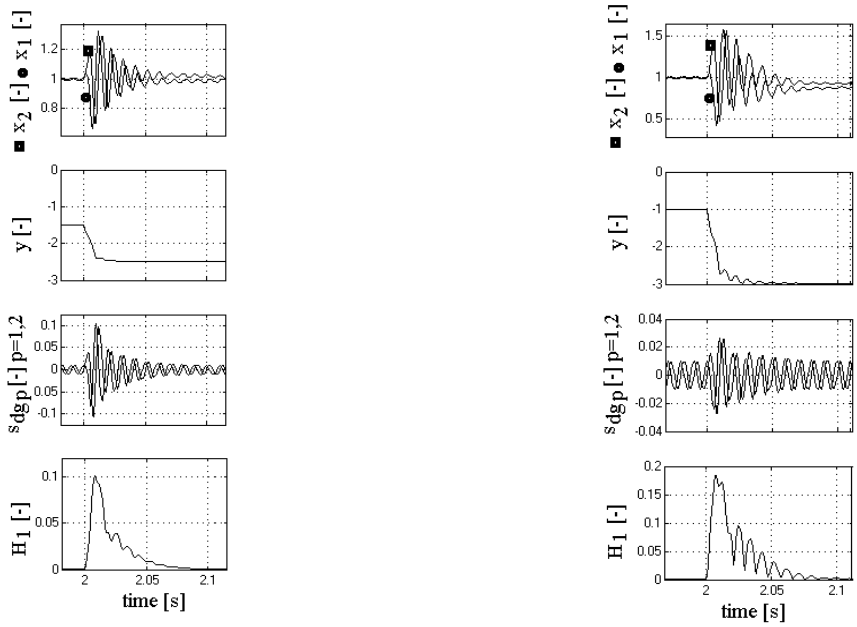

a) $y=\pm 0.5\text{-}2\text{-}(1\text{-}x_1)^2\text{-}(1\text{-}x_2)^2$, $G_{H1}=1$ b) $y=\pm 1\text{-}2\text{-}(1\text{-}x_1)^2\text{-}(1\text{-}x_2)^2$, $G_{H1}=1$

Fig. 11. Zooms of the tracking accuracy for the ESC 2D scheme applied to the perturbed process: $f_d=100$ Hz

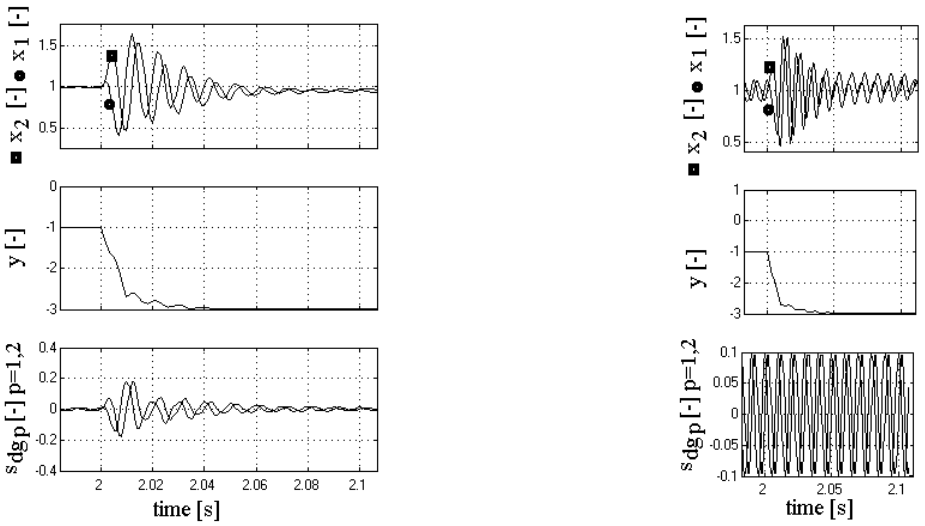

a) bpfESC 2D scheme, $G_{H1}=10$ b) bhoESC 2D scheme ($\beta_{h(bho)}=0.18$, $\beta_{l(bho)}=0.5$)

Fig. 12. Zooms of the tracking accuracy for the ESC 2D scheme applied to the perturbed process: $y=\pm 1\text{-}2\text{-}(1\text{-}x_1)^2\text{-}(1\text{-}x_2)^2$, $f_d=100$ Hz

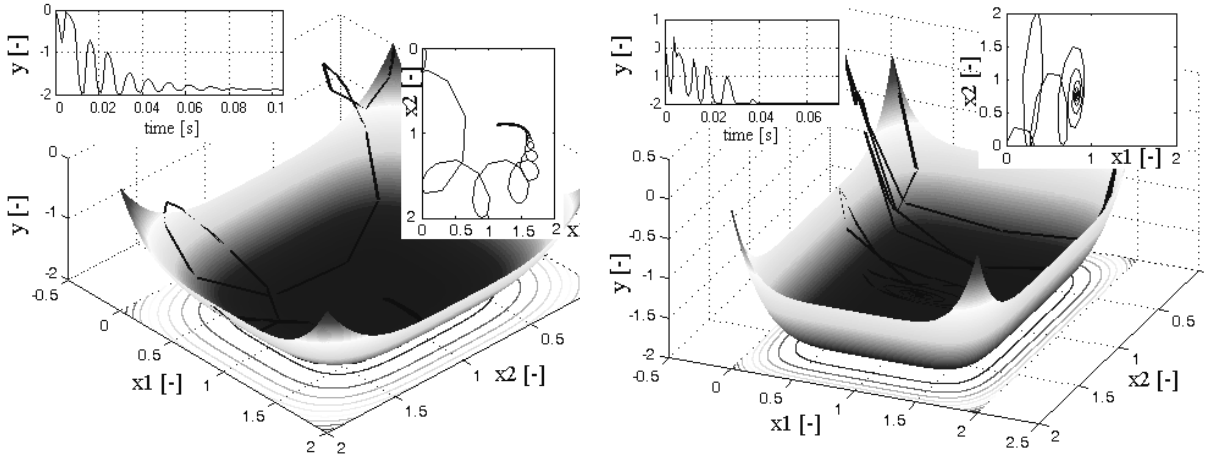

a) applied to the process $y=-2\text{-}(1\text{-}x_1)^4\text{-}(1\text{-}x_2)^4$ b) applied to the process $y=-2\text{-}(1\text{-}x_1)^6\text{-}(1\text{-}x_2)^6$

Fig. 13. The 3D view of the search phase for the ESC 2D scheme ($f_d=100$ Hz)

If the loop gain, k_1, is set proportional to the dither frequency, then the dither persistence is improved [3]. So, if

$$k_1 = \gamma_{sd} \cdot \omega_d \quad (19)$$

then the search speed in the closed loop can be estimated based on

$$K_{SS(p)} = k_{sg(p)} \cdot \gamma_{sd} \cdot \omega_d, \ p = 1, \ 2 \quad (20)$$

Note that $K_{SS(p)}$ indicators are time variables based on relationships (14) and (17).

3.3. Estimation of the search speed in the bhoESC loop

Estimation of the search speed in the closed loop of the bhoESC 2D-scheme can be performed in the same manner if the same assumptions, as above, are considered, excepting that $\beta_{h(bho)}=0.5$.

The LF components in the bhoESC loop are LP filtered, thus only the first harmonic will be considered:

$$x_{LF}(t) = a_1 \sin(\omega_d t + \varphi_1) \quad (21)$$

The signal after the HPF is:

$$s_{HPF}(t) \cong D_1 a_1 \sin(\omega_d t + \varphi_1) \quad (22)$$

Thus, the signal after demodulation can be written as:

$$\begin{aligned} & s_{DM1}(t) = s_{HPF}(t) \cdot \sin(\omega_d t) \cong \\ & \cong \left(D_1 a_1 \cos\varphi_1\right) \cdot \sin^2(\omega_d t) = \\ & = \frac{D_1 a_1 \cos\varphi_1}{2} - \frac{D_1 a_1 \cos\varphi_1}{2} \cdot \cos(2\omega_d t) \end{aligned} \quad (23)$$

Under the assumption mentioned above, the signal after the LPF will be:

$$s_{LPF1}(t) \cong \frac{1}{2} D_1 a_1 \cos\varphi_1 \quad (24)$$

Thus, the signal injected in the loop will be:

$$x_{1(bho)}(t) \cong K_{SS1(bho)} \cdot t + k_2 \sin(\omega_d t) \quad (25)$$

where the search speed is given by:

$$K_{SS1(bho)} = \frac{1}{2} D_1 a_1 k_1 \cos\varphi_1 = \frac{1}{2} D_1 a_1 \gamma_{sd} \omega_d \cos\varphi_1 \quad (26)$$

In the same manner:

$$K_{SS2(bho)} = \frac{1}{2} D_1 a_1 k_1 \sin\varphi_1 = \frac{1}{2} D_1 a_1 \gamma_{sd} \omega_d \sin\varphi_1 \quad (27)$$

4. CONCLUSION

Besides the well known results for the hoESC 1D-scheme that are also available for the bhoESC 2D-scheme (such as the result about the convergence time, which is proportional with the product of the frequency and magnitude of the dither), some new results related to the bpfESC 2D-scheme are shown in this paper. The promising outcomes from this work are listed in the main results: (1) the search speed values was estimated based on the partial derivatives of the unknown DISO map; (2) the differences between the search speed values appear for the bpfESC 2D-scheme based on the use of the BP filter that has an extended frequency band; (3) the dither persistence is dependent to the cut-off frequencies of the BP filter; (4) other performance benefits could arise from the proposed topology for the bpfESC 2D-scheme, which will be exploited in further work.

Note that these advantages must be interpreted in the context of the modeling approach used. The analytical analysis was kept at a simple level in order to gain an initial understanding of the signal processing in the loops of the bpfESC 2D-scheme.

REFERENCES

[1] Ariyur KB, Krstić M. Real-time optimization by extremum-seeking control. John Wiley & Sons, NY 2003.

[2] Azar FE, Perrier M, Srinivasan B. A global optimization method based on multi-unit extremum-seeking for scalar nonlinear systems. Comput Chem Eng 2011;35:456–63.

[3] Bizon N. Energy harvesting from the PV Hybrid Power Source, Energy 2013; 10.1016/j.energy.2013.02.006.

[4] Bizon N. FC energy harvesting using the MPP tracking based on advanced extremum seeking control, International Journal of Hydrogen Energy 2013;38(14):1952-66.

[5] Becherif M, Hissel D. MPPT of a PEMFC based on air supply control of the motocompressor group. Int J Hydrogen Energ 2010; 35(22):12521–30.

[6] Dochain D, Perrier M, Guay M. Extremum seeking control and its application to process and reaction systems: A survey, Mathematics and Computers in Simulation 2011;182(3): 369-80.

[7] Oliveira TR, Peixoto AJ, Hsu L. Global real-time optimization by output-feedback extremum-seeking control with sliding modes. J Franklin Institute 2012;349:1397–415

[8] Moase WH, Manzie C. Fast extremum-seeking for Wiener–Hammerstein plants, Automatica 2012; 48(10):2433–43

[9] Zhang C, Siranosian A, Krstić M. Extremum seeking for moderately unstable systems and for autonomous vehicle target tracking without position measurements. Automatica 2007;43:1832–39

[10] Gelbert G, Moeck JP, Paschereit CO, King R. Advanced algorithms for gradient estimation in one- and two-parameter extremum seeking controllers. J Process Contr 2012;22:700–9.

[11] Ghaffari A, Krstić M, Nešić D. Multivariable Newton-based extremum seeking, Automatica 48 (2012) 1759–1767.

[12] Tan Y, Nešić D, Mareels I. On non-local stability properties of extremum seeking control, Automatica 2006;42:889–903.

[13] Adetola V, Guay M. Parameter convergence in adaptive extremum-seeking control. Automatica 2007;43:105–10.

[14] Tan, Y., Nesic, D., & Mareels, I. (2008). On the choice of dither in extremum seeking systems: a case study. Automatica, 44, 1446–50.

[15] Bizon N. Energy harvesting from the FC stack that operates using the MPP tracking based on modified extremum seeking control, Appl Energ 2013;104:326-36.